Smart Structures and Systems, *Vol. 25, No. 4 (2020) 433-446*
DOI: https://doi.org/10.12989/sss.2020.25.4.433

Numerical simulation of the effect of confining pressure and tunnel depth on the vertical settlement using particle flow code (with direct tensile strength calibration in PFC Modeling)

Hadi Haeri [1], Vahab Sarfarazi*[2] and Mohammad Fatehi Marji [3]

[1] *State Key Laboratory for Deep GeoMechanics and Underground Engineering, Beijing, 100083, China*
[2] *Department of Mining Engineering, Hamedan University of Technology, Hamedan, Iran*
[3] *Mine Exploitation Engineering Department, Faculty of Mining and Metallurgy, Institution of Engineering, Yazd University, Yazd, Iran*

(*Received May 19, 2019, Revised July 28, 2019, Accepted December 21, 2019*)

Abstract. In this paper the effect of confining pressure and tunnel depth on the ground vertical settlement has been investigated using particle flow code (PFC2D). For this perpuse firstly calibration of PFC2D was performed using both of tensile test and triaxial test. Then a model with dimention of 100 m × 100 m was built. A circular tunnel with diameter of 20 m was drillled in the middle of the model. Also, a rectangular tunnel with wide of 10 m and length of 20 m was drilled in the model. The center of tunnel was situated 15 m, 20 m, 25 m, 30 m, 35 m, 40 m, 45 m, 50 m, 55 m and 60 m below the ground surface. these models are under confining pressure of 0.001 GPa, 0.005 GPa, 0.01 GPa, 0.03 GPa, 0.05 GPa and 0.07 GPa. The results show that the volume of colapce zone is constant by increasing the distance between ground surface and tunnel position. Also, the volume of colapce zone was increased by decreasing of confining pressure. The maximum of settlement occurs at the top of the tunnel roof. The maximum of settlement occurs when center of tunnel was situated 15 m below the ground surface. The settlement decreases by increasing the distance between tunnel center line and measuring circles in the ground surface. The minimum of settlement occurs when center of circular tunnel was situated 60 m below the surface ground. Its to be note that the settlement increase by decreasing the confining pressure.

Keywords: direct tensile strength; PFC2D; confining pressure; settlement; tunnel

1. Introduction

A rapid economic development have been presented worldwide due to novel tunnel construction methods in the last 25 years. The huge underground roadways need a lot of excavation works to provide shallow tunnels in relatively soft grounds in urban areas. Therefore, tunneling design and construction methods have been established in the world by imploying the conventional drilling and blasting operations or by using the modern and advanced tunnel boring machines (TBMs). The safetofy conditions, stability and durability of these underground constructions all should be ensured by employing the sophisticated management and engineering design process (Abdollahi *et al*. 2019). A lot of theoretical and numerical researches have been carried out in the field of tunneling design and construction methods. Several numerical studies such as indirect boundary element methods (i.e., displacenment discontinuity and fictitious stress methods) have been developed in recent years to investigate the fracturing patterns related to the rock cutting actions procedures and rock fragmentation mechanisms due to rock blasting and TBM disc cutters performances in the modern mechanized excavation methods (Hosseini_Nasab *et al*. 2007, Marji *et al*. 2009, Lak *et al*. 2019, Marji 2015, Nikaadat and Marji 2016, Haeri and Marji 2016). One of the main issues in these huge manmade underground roadways is the surface subsidence phenoma resulting from the vertical and lateral movements of the relatively soft grounds surrounding these structures (e.g., Peck 1969, Attewell and Yates 1984, and Mair and Taylor 1997, Boscardin and Cording 1989, Ou *et al*. 2008, Yoo and Lee 2008, Nabil *et al*. 2012, Bi *et al*. 2016, Ramadoss and Nagamani 2013, Pan *et al*. 2014, Panaghi *et al*. 2015, Haeri 2015, Haeri and Sarfarazi 2016, Haeri *et al*. 2015, 2016, Monfared 2017, Boumaaza *et al*. 2017, Zhou and Bi 2018).

A critical threat to both surface and subsurface facilities may be the soft ground movements in urban areas which should be predicted before the construction and controlled during and after its completion (Papastamos *et al*. 2014, Wu *et al*. 2015, Zhang *et al*. 2015, Liao *et al*. 2009).

The shallow depth and soft ground are the two major charactteristics of the near surface tunneling projects which may result in considerable subsidence phenomenon (Dindarloo and Siami-Irdemoosa 2015, Mirsalari *et al*. 2017). The tunneling induced ground subsidence can be analyzed, forcasted and controlled through a sound engineering design of any tunneling projects. Thus, subsidence phenomenon is one of the major concerns in many urban underground structures because of their relatively shallow depths and their safety issues in the

*Corresponding author, Assistant Professor,
E-mail: vahab.sarfarazi@gmail.com

http://www.techno-press.org/?journal=sss&subpage=7 ISSN: 1738-1584 (Print), 1738-1991 (Online)

populated cities. The prediction of the magnitude and duration of the vertical and horizontal movements of the ground surfaces above the underground tunnels can be of main concerns in tunnel engineering. A lot of impirical, analytical, numerical and artificial intelligence methods have been imployed by many researchers to predict the maximum ground subsidence induced by a shallow tunnel (O'Reilly and New 1982, Peck 1969, Bobet 2001, Loganathan and Poulos 1998, Kasper and Meschke 2004, Melis *et al*. 2002, Neaupane and Adhikari 2006, Suwansawat and Einstein 2006, Wang *et al*. 2013). Although, several advantages are being gained from these studies for predicting the tunnel induced subsidence, most of these methods need some assumptions and simplications (constrains) to be able to solve the problem. For example, in most cases, in the analytical and numerical solutions of three dimensional subsidence problems, the plain strain condition is assumed (Chou and Bobet 2002), the elastic behavior is stablished (Park 2004), and the rock and soil isotropy conditions are taken into account (Franzius *et al*. 2005).

The prediction and assessment of ground subsidence due to tunnel excavation may ensure the construction safety performance of this shallow subsurface structure. Therefore, the surface subsidence phenomena and their safety issues in shallow tunneling industry remains a big engineering chalenge which is rarely studied. In the soft grounds, the deformation and failure process of shallow excavations such as tunnels have been considered as the basic engineering concerns and therefore, a plenthy of research works has been devoted to this important task (Broms and Bennermark 1967, Peck 1969, Davis *et al*. 1980, Clough *et al*. 1983, Lee *et al*. 2006, Adachi *et al*. 2003, Chakeri *et al*. 2013, Chakeri and Ünver 2014, Wan *et al*. 2016, Goh *et al*. 2017).

Although several experimental and field measurement tests were developed to investigate and solve many rock engineering problems, the model tests accompanying with the theoretical and numerical methods such as finite element, boundary element and finite difference methods have also been devoted and used form augmenting and completing the overall solutions of these problems. However, for the discontinuum soil and rock masses where large deformations theories are of main concern, the continuum based methods (such as finite and boundary element methods) in some cases may not be able to reflect the discrete characteristics of the geo-materials. Therefore, the discrete element method (DEM) may be considered as a proper alternative to reflect the mechanical behavior of rock-like materials encountered in any tunnel construction

(a)

(b)

(c)

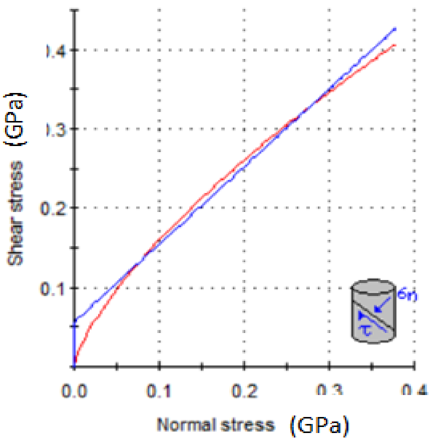

(d)

Fig. 1 (a) The Universal Tensile Testing Machine (UTTM); (b) granite sample; (c) granite sample; (d) shear stress versus normal stress project. Thus, in the present study, the DEM based particle flow code in two dimensions (PFC2D) is used to be able to simulate the discontinuum nature, large deformation behaviour and cracks propagation process in geo-materials. Cundall (Cundall 1971, Cundall and Strack 1979) originally developed the explicit finite difference method known as DEM. His work was rapidly and widely used in geotechnical engineering (Rothenburg and Bathurst 1989, Oda and Kazama 1998, Cai *et al*. 2007, Ng *et al*. 2013). However, in this paper, the effects of confining pressures and tunnel depths on the surface subsidence have been studied by using a sophisticated computer code based on DEM.

2. Experimantal test

2.1 Direct tensile strength test by compressive-to-tensile load convertor (CTLC) device

In this study, a Universal Tensile Testing device (UTTM) is developed as shown in Fig. 7. The CTLC device together with granite specimens already prepared in the laboratory can be used to complete the required arrangement for measuring the direct tensile strength of the granite (Fig. 7). In this experimental approach, the UTTM have a conventional uniaxial compression frame which can provide the required uniaxial compression for the CTLC device already contained a granite specimen. The loading frame of UTTM is specially designed for applying a uniaxial compressive load to the end plates of the CTLC device via a 5-tons gearbox load cell which can electronically record the applied load increments during tensile testing process. During the testing operation, a constant loading rate of 0.02 MPa/s is applied to minimize its effects on the final testing results of the direct tensile strength of granite specimen. This loading rate is suggested for the tensile strength measurement using a rock splitting approach. UTTM is powered by a single-phase electricity applying through a rigid frame of 5 tons loading capacity and can be effectively used for measuring the direct and indirect tensile strengths, the uniaxial compressive and the fracture toughness's of concretes, rocks, ceramics, mortars and asphalts. However, UTTM cannot be used for measuring the uniaxial strength of relatively hard rocks but it can be used for measuring the compressive strength of rock like materials, soft and medium rocks, ceramics and asphalts, successfully.

In the present research, the UTTM with CTLC device is used to measure the direct tensile strength of granite specimens. Therefore, 15 pre-holed rectangular specimens of granite are prepared and placed in the CTLC device for testing with UTTM in a rock mechanics laboratory. Figs. 1(b) and (c) show the failure and crack propagation process in 2 failed specimens. These figures show that when the granite specimens are subjected to tensile loading the horizontal line cracks are getting started from the boundary of the center holes and extend through the specimens' width. This is the direct tensile failure causing the splitting tensile failure to be produced by the semi-cylindrical steels or rings around the periphery of the central hole in the specimen. The value of tensile strength has been depicted in Table 2.

2.2 Triaxial test on the granite

Cuncurent with tensile strength, triaxial test have been done on the granite specimens. Fig. 1(d) shows Shear stress versus normal stress for granite specimen. The value of cohesion and friction angle has been depicted in Table 2.

3. Numerical simulation of the subsidence phenomena in shallow tunnels

The subsidence phenomena in shallow tunneling projects can be predicted by using the two dimensional particle flow code (PFC2D). In this work, the effect of tunnel depths and confining pressures on the surface subsidence due to shallow tunnel excavation are numerically simulated analyzed.

3.1 Particle Flow Code in Two Dimensions (PFC2D) and Bonded Particle Model (BPM)

A discrete element code developed by Itasca 1999 (version 3.1) and improved by Potyondy and Cundall (20014) known as particle flow code in two dimensions (PFC2D) is used in this study to investigate the effects of tunnel depths and confining pressures on the surface subsidence of a typical shallow tunnel excavated in a soft (soil) ground. In this computer code, the interactions forces and the relative movements of the material particles within an assembly are computed using an explicit central finite difference method (FDM) known as discrete element method (DEM). A bonded particle model (BPM) algorithm is adopted in PFC2D to model the contact conditions of the particles within the material's particles assembly. The two linear and non-linear contact models taking into account the frictional sliding of the particles can be used. In the linear contact model an elastic relationship is established between the contact forces and the particle's relative displacements. A parallel-bonded particle model can be generated for PFC2D by using the routines suggested by Itasca 1999; version 3.1.

In this modelling procedure, the following micro-mechanical properties should be defined for any particular particle assembly: (i) the ball-to-ball contact modulus; (ii) the stiffness ratio Kn/Ks; (iii) the friction coefficients of balls; (iv) the normal and shear parallel bond strengths,; (v) the standard deviation of the mean bonding strength considering both normal and shear strengths of the bond; (vi) the minimum ball radius; (vii) the radius multiplier, stiffness raio and modulus of the parallel bond. A standard calibration procedure is adopted in PFC2D to provide the appropriate micro properties for each particle assembly model. However, the bonding characteristics and contact properties for the particles in an assembly cannot be directly measured from the laboratory experimental results gained from the real geo-material samples. The macro-mechanical properties of the material samples can be measured through laboratory tests based on their continuum behavior. To

Table 1 Micro properties used to represent the intact rock

Parameter	Value	Parameter	Value
Type of particle	disc	Stiffness ratio	2
Density (Kg/cm3)	3600	Particle friction coefficient	0.5
Minimum radius (mm)	0.27	Contact bond normal strength, mean (GPa)	0.2
Size ratio	1.56	Contact bond normal strength, SD (GPa)	0.04
Porosity ratio	0.08	Contact bond shear strength, mean (GPa)	0.2
Damping coefficient	0.7	Contact bond shear strength, SD (GPa)	0.04
Contact young modulus (GPa)	10		

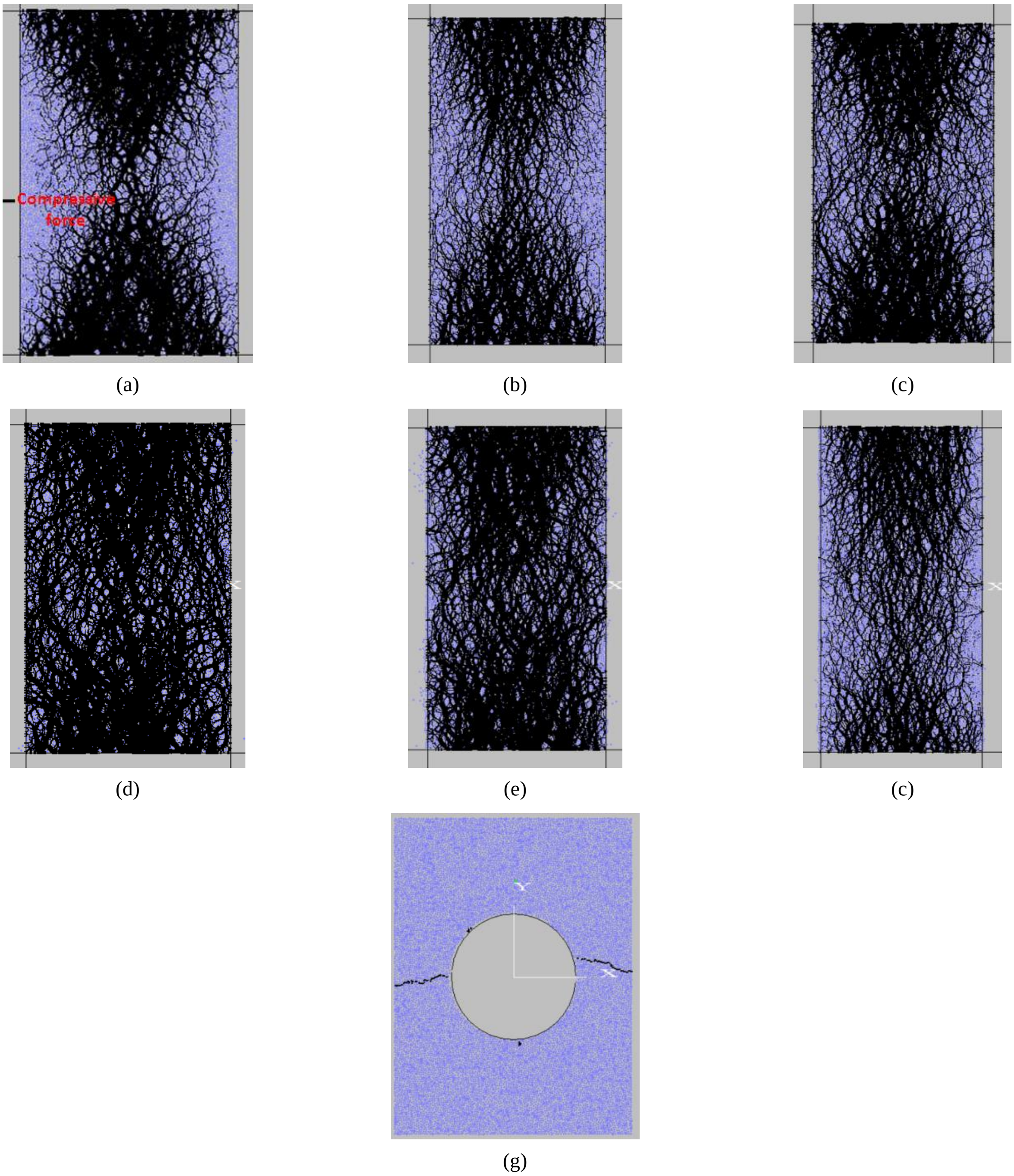

Fig. 2 Contact force in models under different confining pressure of (a) 0.001 Gpa; (b) 0.005 Gpa; (c) 0.01 Gpa; (d) 0.03 Gpa; (e) 0.05 Gpa; (f) 0.07 Gpa; (g) failure pattern of numerical model

Table 2 Direct tensile strengths of physical sample and numerical model

	Experimental test	Numerical simulation
Cohesion (GPa)	0.05	0.056
Friction angle (°)	42	44.5
Tensile strength (MPa)	6.5	7

estimate the appropriate micro-properties of the modeled samples from the real macro-properties obtained from experimental tests, an inverse modeling procedure is adopted I n PFC2D. This method is the versatile trial and error approach which relates these two sets of materials properties (PFC 2D 1999). The trial and error algorithm assumes the micro-mechanical property values at the first step and then compares the strength and deformation characteristics of the numerical models with those measured form the laboratory tests. By an iterative process, the appropriate micro-mechanical properties of the modeled samples can be achieved. The limitations of DEM are as follow: (a) Fracture is closely related to the size of elements, and that is so called size effect. (b) Cross effect exists because of the difference between the size and shape of elements with real grains. (c) In order to establish the

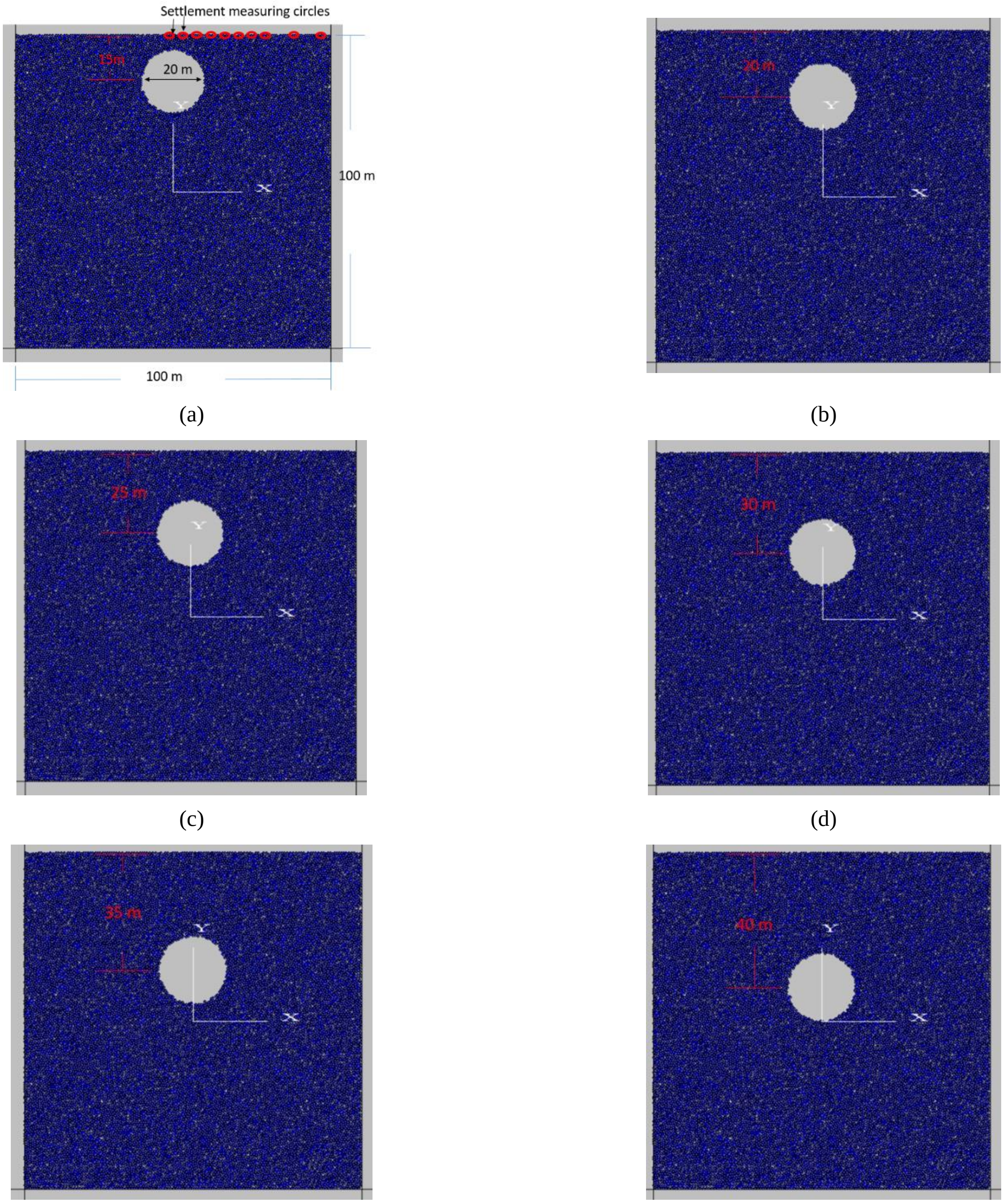

(a) (b) (c) (d) (e) (f)

Fig. 3 Numerical models with circular tunnel; The center of circular tunnel was situation in 10 different positions below the ground surface of (a) 15 m; (b) 20 m; (c) 25 m; (d) 30 m; (e) 35 m; (f) 40 m; (g) 45 m; (h) 50 m; (i) 55 m and (j) 60 m

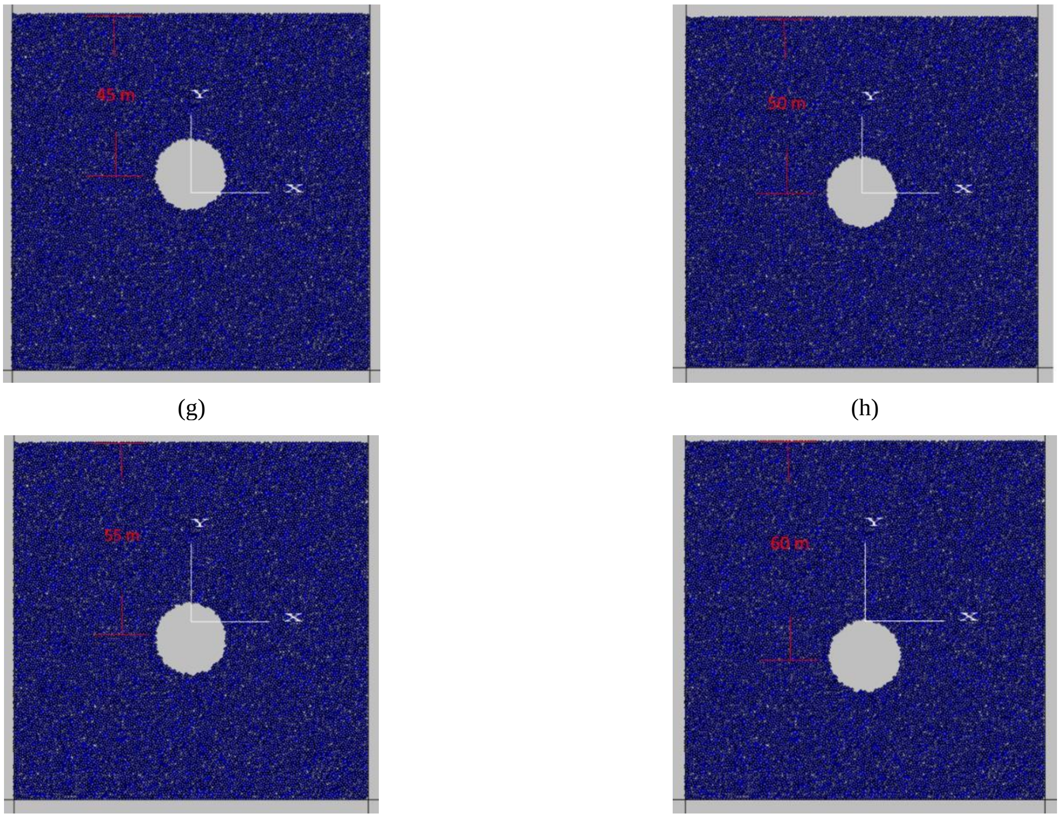

(g) (h)

(i) (j)

Fig. 3 Continued

relationship between the local and macroscopic constitutive laws, data obtained from classical geomechanical tests which may be impractical are used.

3.2 Preparing and calibrating the numerical model

The triaxial compression test was used to calibrate the cohesion and friction angle of specimen in PFC2D model. The standard process of generation of a PFC2D assembly to represent a test model involves four steps: (a) particle generation and packing the particles, (b) isotropic stress installation, (c) floating particle elimination, and (d) bond installation.

Adopting the micro-properties listed in Table 1 and the standard calibration procedures (Potyondy and Cundall 2003), a calibrated PFC particle assembly was created. The dimension of the tri-axial model were 54 mm and 108 mm. The specimen was made of 15,615 particles. The lateral walls were moved toward each other in a servo control manner to reach desirable confining pressure i.e., 0.001 GPa, 0.005 GPa, 0.01 GPa, 0.03 GPa, 0.05 GPa and 0.07 GPa, respectively. The upper and lower walls was moved toward each other with a low speed of 0.016 m/s. Fig. 2 illustrate the contact force chain of the numerical tested samples for six different confining pressure. The contact force chain is like a cone shape when model is tested under low confining pressure and contact force chain are distributed in all of the model by increasing the confining pressure. Fig. 1(d) shows Mohr-Coloumb envelope in these data. The cohesion and friction angle were gained by this envelope. These shear properties are well matching with those of experimental test (Table 2). This shows that model is calibrated correctly.

Its to be note that CTLC test was simulated for calibration of tensile strength of model. Table 2 gives the numerical values of the direct tensile strengths obtained by PFC2D. Comparing these results with those obtained experimentally in Table 2. One can easily visualize that these two set of direct tensile strength values are very close to each other which again the validity of both experimental and numerical procedures adopted in this study is approved. Fig. 2(g) shows the failure pattern of model under direct tensile test. A good agreement was established between experimental test and numerical simulation.

3.3 Model preparation using particle flow code

After calibration of PFC2D, a rectangular model consisting a circular tunnel was built. Dimension of rectangular model was 100 m × 100 m. The diameter of tunnel was 20 m. the center of tunnel was situation in 10 different positions below the surface i.e., 15 m, 20 m, 25 m, 30 m, 35 m, 40 m, 45 m, 50 m, 55 m and 60 m, respectively (Fig. 3). A total of 14,179 disks with a minimum radius of 0.27 cm were used to make up the rectangular specimen. Rectangular models are under confining pressures of 0.001 GPa, 0.005 GPa and 0.01 GPa. These models are loaded gravitationally. For measurement of ground settlement, 15 circles with diameter of 2 m were chosen on the surface and the average of vertical displacement of discs surounded in

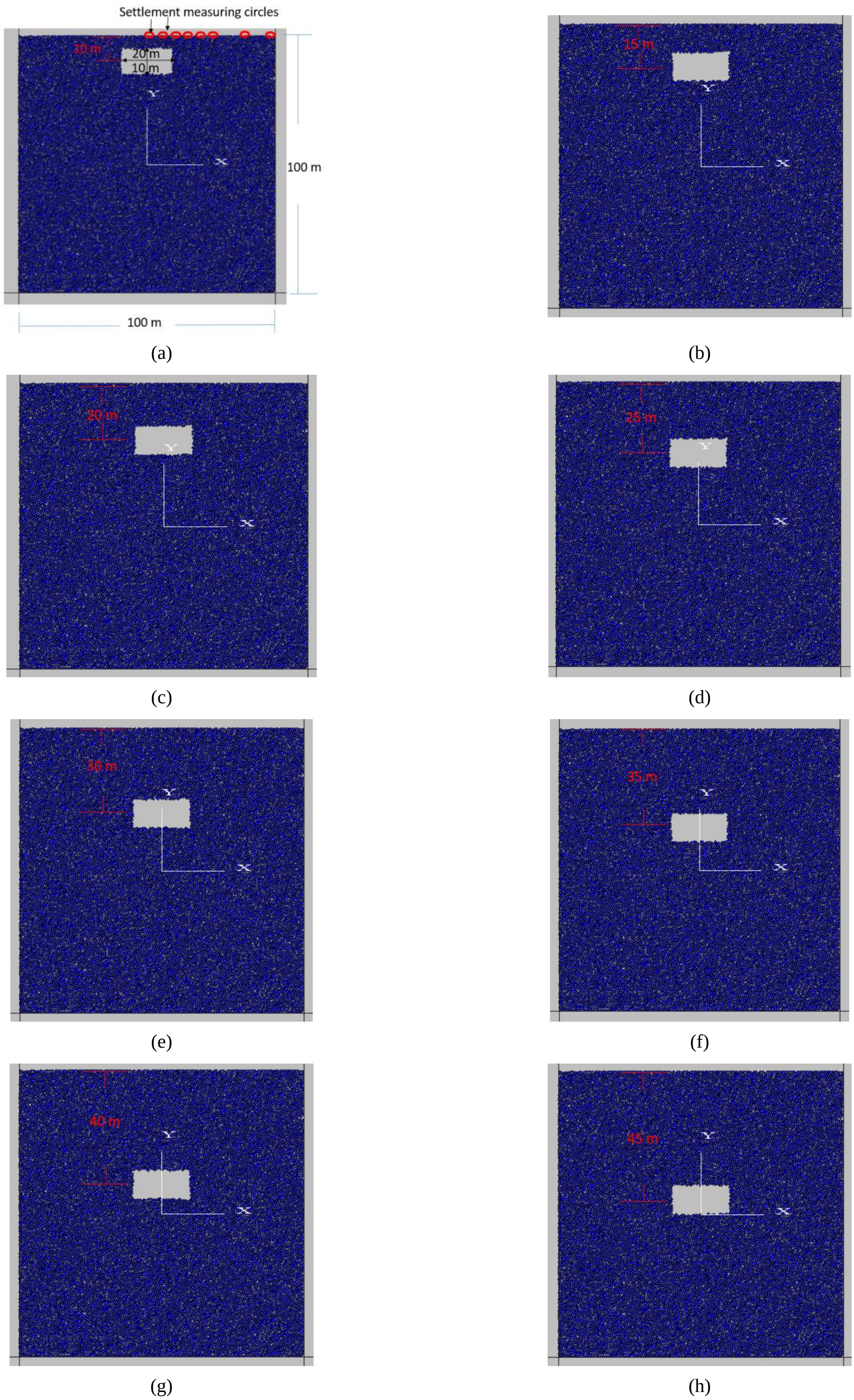

Fig. 4 Numerical models with circular tunnel; The center of circular tunnel was situation in 10 different positions below the ground surface of (a) 10 m; (b) 15 m; (c) 20 m; (d) 25 m; (e) 30 m; (f) 35 m; (g) 40 m; (h) 45 m; (i) 50 m and (j) 55 m

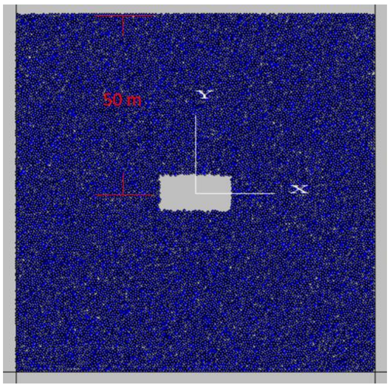

(i)

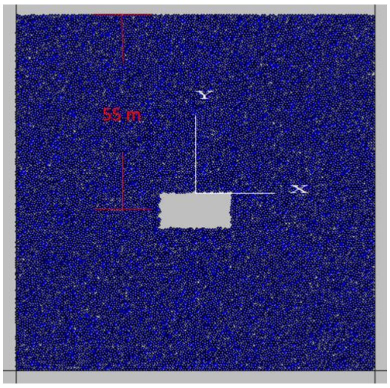

(j)

Fig. 4 Continued

these circles was chosen as a ground settlement (Fig. 3(a)).

(a) Models under confining pressure of 0.001 GPa:

When center of tunnel is situated 15 m, 20 m, 25 m, 30 m, 35 m, 40 m, 45 m, 50 m, 55 m and 60 m below the surface (Fig. 4), a wedge of particle colapcse inside the tunnel. The size of these wedge is constant by increasing the distance between tunnel center and ground surface. Its to be note that the particles of side wall of tunnel were fixed in the place.

(b) Models under confining pressure of 0.005 GPa:

When center of tunnel is situated 15 m, 20 m, 25 m, 30 m, 35 m, 40 m, 45 m, 50 m, 55 m and 60 m below the surface (Fig. 5), a wedge of particle colapcse inside the tunnel. The size of these wedge is constant by increasing the distance between tunnel center and ground surface. Its to be note that the particles of side wall of tunnel were fixed in the place.

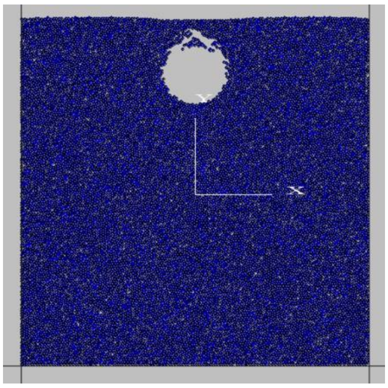

(a)

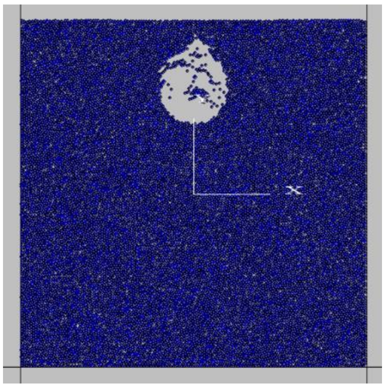

(b)

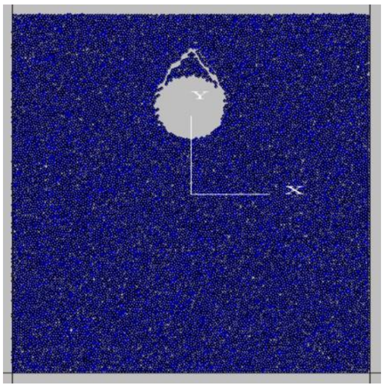

(c)

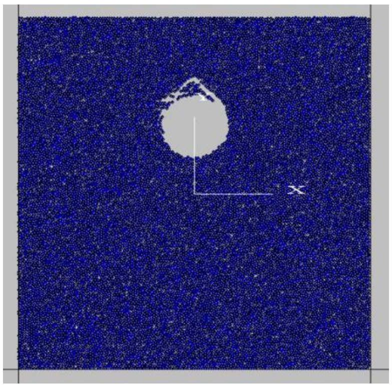

(d)

Fig. 5 Failure pattern in numerical models; The center of circular tunnel was situation below the ground surface of (a) 15 m; (b) 20 m; (c) 25 m; (d) 30 m; (e) 35 m; (f) 40 m; (g) 45 m; (h) 50 m; (i) 55 m and (j) 60 m

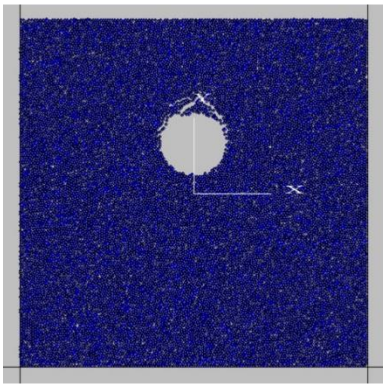

(e)

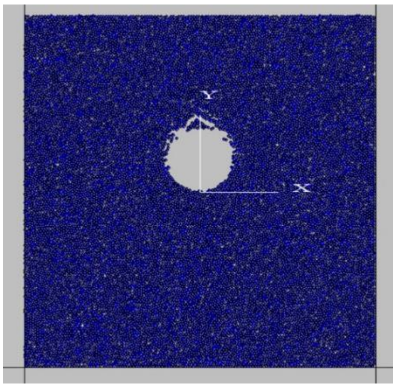

(f)

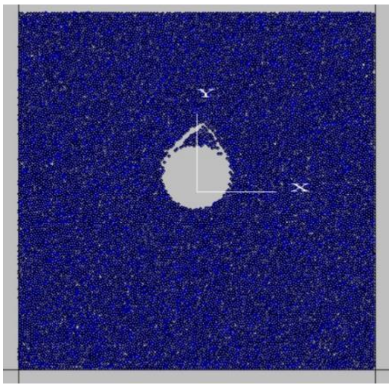

(g)

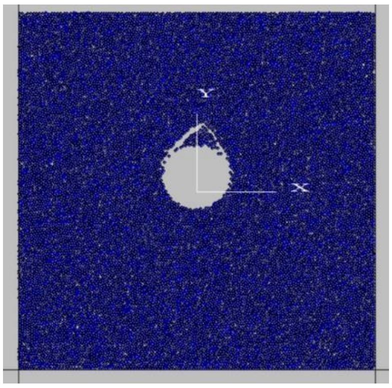

(h)

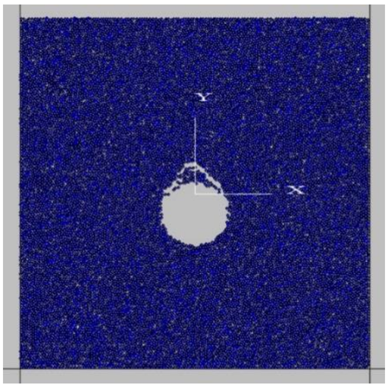

(i)

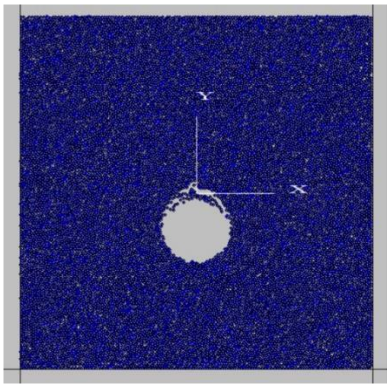

(j)

Fig. 5 Continued

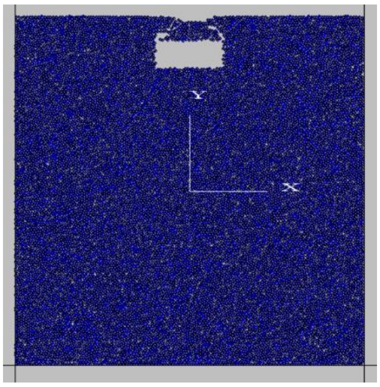

(a)

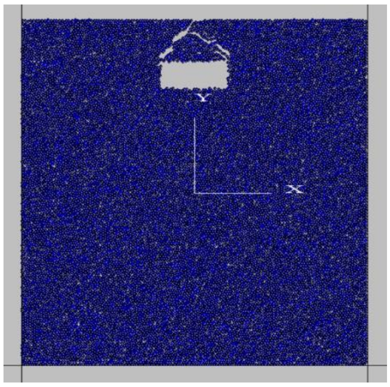

(b)

Fig. 6 Failure pattern in numerical models; The center of circular tunnel was situation below the ground surface of (a) 10 m; (b) 15 m; (c) 20 m; (d) 25 m; (e) 30 m; (f) 35 m; (g) 40 m; (h) 45 m; (i) 50 m; (j) 55 m

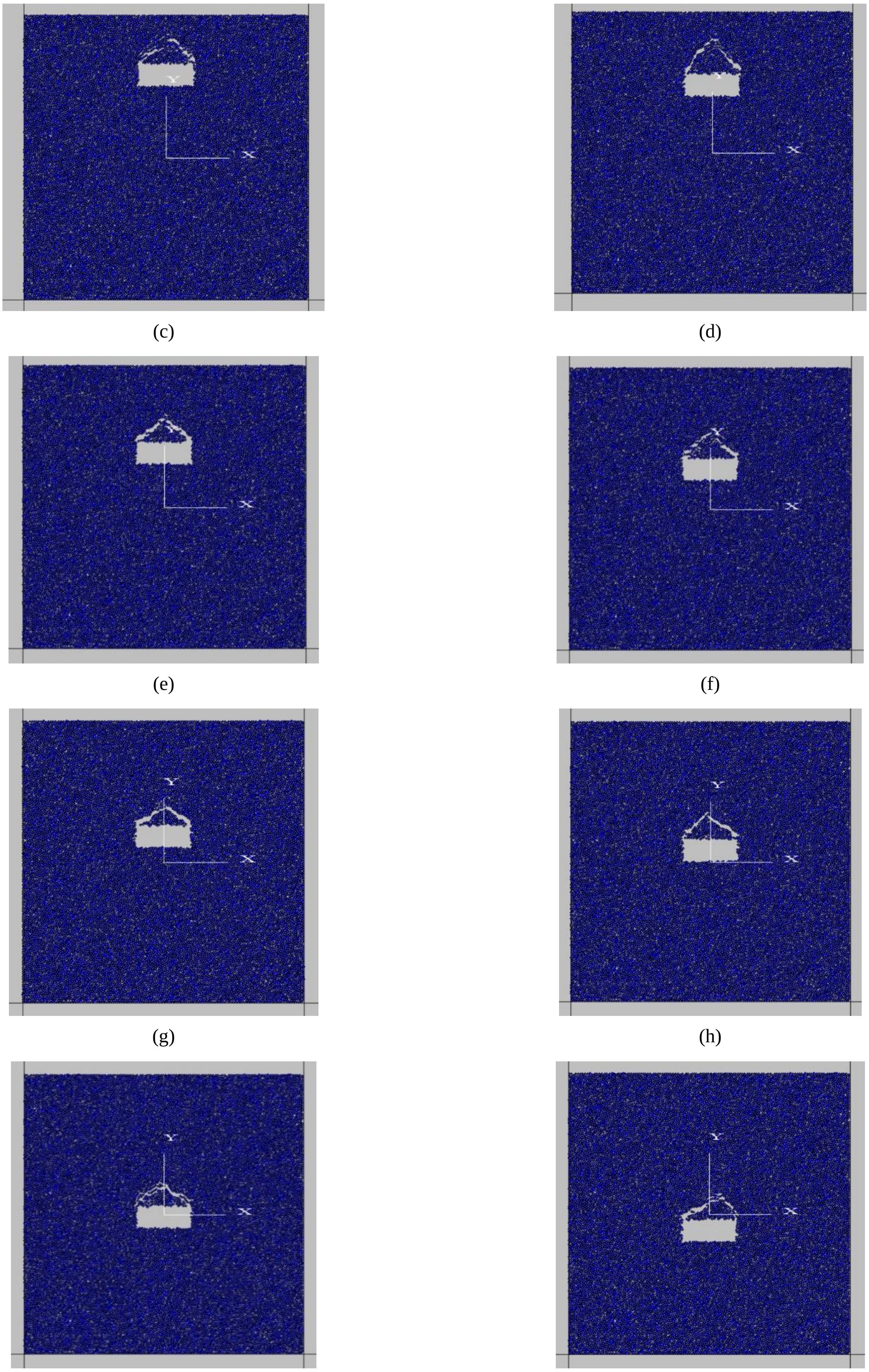

(c) (d) (e) (f) (g) (h) (i) (j)

Fig. 6 Continued

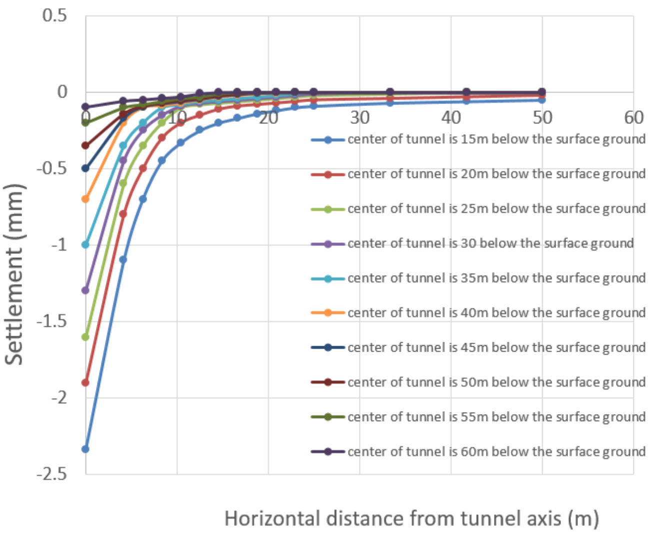

Fig. 7 The settlement diagram for circular tunnel under confining pressure of 0.001 GPa

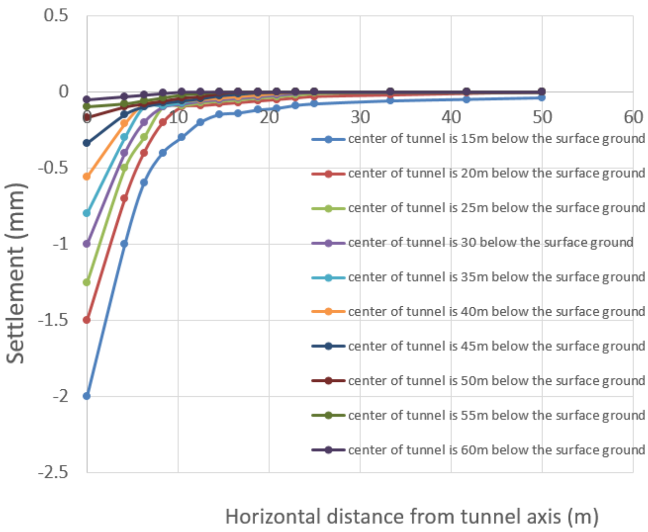

Fig. 8 The settlement diagram for circular tunnel under confining pressure of 0.005 GPa

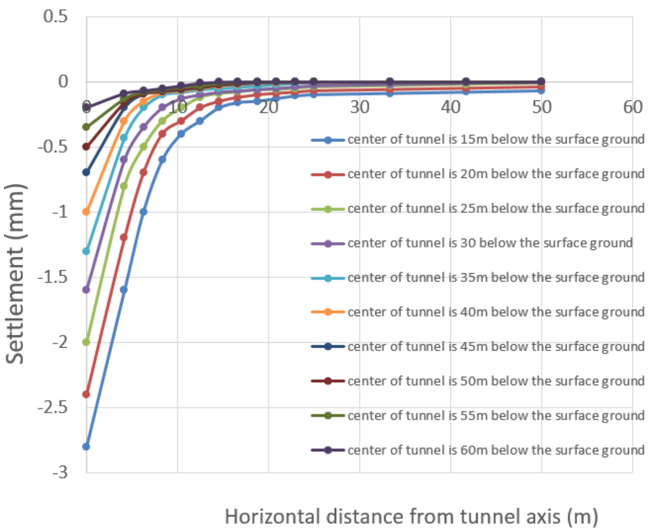

Fig. 9 The settlement diagram for circular tunnel under confining pressure of 0.01 GPa

(c) Models under confining pressure of 0.01 GPa:

When center of tunnel is situated 15 m, 20 m, 25 m, 30 m, 35 m, 40 m, 45 m, 50 m, 55 m and 60 m below the surface (Fig. 6), several groups of particles colapcse inside the tunnel. The size of these groups is constant by increasing the distance between tunnel center and ground surface. Its to be note that the particles of side wall of tunnel move inside the tunnel. From Figs. 4, 5 and 6, its clear that the volume of failure zone increase by decreasing the confining pressure.

4. Comparison of settlement diagram for circular tunnel under three different confining pressure

Figs. 7, 8 and 9 show the settlement diagram for circular tunnel under confining pressure of 0.001 GPa, 0.005 GPa, and 0.01 GPa, respectively. Totally the ground settlement has maximum value when confining pressure was 0.01 GPa. From Figs. 7, 8 and 9, it's clear that the maximum of settlement occurs at the top of the tunnel roof in the ground surface. The maximum of settlement occurs when center of tunnel was situated 15 m below the ground surface. Its amount was 2 mm, 2.33 mm and 2.8 mm for confining pressure of 0.001 GPa, 0.05 GPa and 0.01 GPa. The settlement decreases by increasing the distance between tunnel center line and measuring circles in the ground surface. The minimum of settlement occurs when center of circular tunnel was situated 60 m below the surface ground.

5. Conclusions

In this paper the effect of confining pressure and tunnel depth on the ground vertical settlement has been investigated using PFC2D. for this perpuse firstly calibration of PFC2D was performed using triaxial test. Then a model with dimention of 100 m × 100 m was built. a circular tunnel with diameter of 20 m was drillled in the middle of the model. The center of circular tunnel was situated 15 m, 20 m, 25 m, 30 m, 35 m, 40 m, 45 m, 50 m, 55 m and 60 m. these models are under confining pressure of 0.001 GPa, 0.005 GPa and 0.01 GPa. the results show that:

- A wedge of particle colapcse inside the tunnel in lower confining pressure. Several groups of particles move inside the tunnel by increasing the confining pressure. Also, several balls from side walls of tunnel move inside the tunnel in high cnfining pressure. The size of colapse zone are decrease by increasing the confining pressure.
- Totally the ground settlement has maximum value in low confining pressure.
- It's clear that the maximum of settlement occurs at the top of the tunnel roof in the ground surface.
- The maximum of settlement occurs when center of tunnel was situated 15 m below the ground surface. Its amount was 2 mm, 2.33 mm and 2.8 mm for confining pressure of 0.001 GPa, 0.005 GPa and 0.01 GPa, respectivly.
- The settlement decreases by increasing the distance between tunnel center line and measuring circles in the ground surface.
- The minimum of settlement occurs when center of circular tunnel was situated 60 m below the surface ground.
- The circular shape of tunnel change to non-circular by increasing the confining pressure.

References

Abdollahi, M.S., Najafi, M., Bafghi, A.Y. and Marji, M.F. (2019), “A 3D numerical model to determine suitable reinforcement strategies for passing TBM through a fault zone, a case study: Safaroud water transmission tunnel”, *Iran Tunnel. Undergr. Space Technol.*, **88**, 186-199. https://doi.org/10.1016/j.tust.2019.03.008

Adachi, T., Kimura, M. and Kishad, K. (2003), “Experimental study on the distribution of earth pressure and surface settlement through three-dimensional trapdoor tests”, *Tunnel. Undergr. Space Technol.*, **18**(2-3), 171-183. https://doi.org/10.1016/S0886-7798(03)00025-7

Attewell, P.B. and Yeates, J. (1984), *Ground Movements and their Effects on Structures*, Blackie and Son Ltd., Attewell, P.B. and Taylor, R.K.

Bi, J., Zhou, X.P. and Qian, Q.H. (2016), “The 3D numerical simulation for the propagation process of multiple pre-existing flaws in rock-like materials subjected to biaxial compressive loads”, *Rock Mech. Rock Eng.*, **49**(5), 1611-1627. https://doi.org/10.1007/s00603-015-0867-y

Bobet, A. (2001), “Analytical solutions for shallow tunnels in saturated ground”, *J. Eng. Mech.*, **127**(12), 1258-1266. https://doi.org/10.1061/(ASCE)0733-9399(2001)127:12(1258)

Boscardin, M.D. and Cording, E.J. (1989), “Building response to excavation-induced settlement”, *J. Geotech. Eng.*, **115**(1), 1-21. https://doi.org/10.1061/(ASCE)0733-9410(1989)115:1(1)

Boumaaza, M., Bezazi, A., Bouchelaghem, H., Benzennache, N., Amziane, S. and Scarpa, F. (2017), “Behavior of pre-cracked deep beams with composite materials repairs”, *Struct. Eng. Mech., Int. J.*, **63**(4), 43-56. https://doi.org/10.12989/sem.2017.63.5.575

Broms, B.B. and Bennermark, H. (1967), “Stability of clay at vertical openings”, *J. Soil Mech. Found. Div.*, **93**, 71-94.

Cai, M., Kaiser, P.K., Morioka, H., Minami, M. and Maejima, T. (2007), “FLAC/PFC coupled numerical simulation of AE in large-scale underground excavations”, *Int. J. Rock Mech. Mining Sci.*, **44**(4), 550-564. https://doi.org/10.1016/j.ijrmms.2006.09.013

Chakeri, H. and Ünver, B. (2014), “A new equation for estimating the maximum surface settlement above tunnels excavated in soft ground”, *Environ. Earth*, **71**(7), 3195-3210. https://doi.org/10.1007/s12665-013-2707-2

Chakeri, H., Ozcelik, Y. and Unver, B. (2013), “Effects of important factors on surface settlement prediction for metro tunnel excavated by EPB”, *Tunnel. Undergr. Space Technol.*, **36**, 14-23. https://doi.org/10.1016/j.tust.2013.02.002

Chou, W.-I. and Bobet, A. (2002), “Predictions of ground deformations in shallow tunnels in clay”, *Tunnel. Undergr. Space Technol.*, **17**(1), 3-19. https://doi.org/10.1016/S0886-7798(01)00068-2

Clough, G.W., Sweeney, S.P. and Finno, R.J. (1983), “Measured soil response to EPB shield tunneling”, *J. Geotech. Geoenviron. Eng.*, **109**(2), 131-149. https://doi.org/10.1061/(ASCE)0733-9410(1983)109:2(131)

Cundall, P.A. (1971), “A computer model for simulating progressive large scale movements in blocky rock systems", *Proceeding of the Symposium of the International Society for Rock Mechanics*, Nancy, France, Vol. 1, No. 8.

Cundall, P.A. and Strack, O.D.L. (1979), "A discrete numerical model for granular assemble", *Geotechnique*, **29**(1), 47-65. https://doi.org/10.1680/geot.1979.29.1.47

Davis, E.H., Gunn, M.J., Mair, R.J. and Seneviratne, H.N. (1980), "The stability of shallow tunnels and underground openings in cohesive material", *Geotechnique*, **30**(4), 397-416. https://doi.org/10.1680/geot.1980.30.4.397

Dindarloo, S.R. and Siami-Irdemoosa, E. (2015), "Maximum surface settlement based classification of shallow tunnels in soft ground", *Tunnel. Undergr. Space Technol.*, **49**(1), 320-327. https://doi.org/10.1016/j.tust.2015.04.021

Franzius, J., Potts, D. and Burland, J. (2005), "The influence of soil anisotropy and K_0 on ground surface movements resulting from tunnel excavation", *Géotechnique*, **55**(3), 189-199. https://doi.org/10.1680/geot.2005.55.3.189

Goh, A.T.C., Zhang, W.G., Zhang, Y.M., Xiao, Y. and Xiang, Y.Z. (2017), "Determination of EPB tunnelrelated maximum surface settlement: A multivariate adaptive regression splines approach", *Bull. Eng. Geol. Environ.*, **77**, 489-500. https://doi.org/10.1007/s10064-016-0937-8

Haeri, H. (2015), "Simulating the crack propagation mechanism of pre-cracked concrete specimens under shear loading conditions", *Strength Mater.*, **47**(4), 618-632. https://doi.org/10.1007/s11223-015-9698-z

Haeri, H. and Marji, M.F. (2016), "Simulating the crack propagation and cracks coalescence underneath TBM disc cutters", *Arab. J. Geosci.*, **9**(2), 124. https://doi.org/10.1007/s12517-015-2137-4

Haeri, H. and Sarfarazi, V. (2016), "The effect of non-persistent joints on sliding direction of rock slopes", *Comput. Concrete, Int. J.*, **17**(6), 723-737. https://doi.org/10.12989/cac.2016.17.6.723

Haeri, H., Khaloo, A. and Marji, M.F. (2015), "Experimental and numerical simulation of the microcrack coalescence mechanism in rock-like materials", *Strength Mater.*, **47**(5), 740-754. https://doi.org/10.1007/s11223-015-9711-6

Haeri, H., Sarfarazi, V. and Hedayat, A. (2016), "Suggesting a new testing device for determination of tensile strength of concrete", *Struct. Eng. Mech., Int. J.*, **60**(6), 939-952. https://doi.org/10.12989/sem.2016.60.6.939

Hosseini_Nasab, H. and Fatehi Marji, M. (2007), "A semi-infinite higher-order displacement discontinuity method and its application to the quasistatic analysis of radial cracks produced by blasting", *J. Mech. Mater. Struct.*, **2**(3), 439-458. https://doi.org/10.2140/jomms.2007.2.439

Kasper, T. and Meschke, G. (2004), "A 3D finite element simulationmodel for TBM tunnelling in soft ground", *Int. J. Numer. Anal. Methods Geomech.*, **28**(14), 1441-1460. https://doi.org/10.1002/nag.395

Lak, M., Marji, M.F., Bafghi, A.Y. and Abdollahipour, A. (2019), "Analytical and numerical modeling of rock blasting operations using a two-dimensional elasto-dynamic Green's function", *Int. J. Rock Mech. Mining Sci.*, **114**, 208-217. https://doi.org/10.1016/j.ijrmms.2018.12.022

Lee, C.J., Wu, B.R. and Chen, H.T. (2006), "Tunnel stability and arching effects during tunneling in soft clayey soil", *Tunnel. Undergr. Space Technol.*, **21**(2), 119-132. https://doi.org/10.1016/j.tust.2005.06.003

Liao, S.-M., Liu, J.-H., Wang, R.-L. and Li, Z.-M. (2009), "Shield tunneling and environment protection in Shanghai soft ground", *Tunnel. Undergr. Space Technol.*, **24**(4), 454-465. https://doi.org/10.1016/j.tust.2008.12.005

Loganathan, N. and Poulos, H. (1998), "Analytical prediction for tunneling-induced ground movements in clays", *J. Geotech. Geoenviron. Eng.*, **124**(9), 846-856. https://doi.org/10.1061/(ASCE)1090-0241(1998)124:9(846)

Mair, R.J. (1979), "Centrifugal Modelling of Tunnel Construction in Soft Clay", Ph.D. Thesis; Cambridge University.

Mair, R.J. and Taylor, R.N. (1997), "Bored tunnelling in the urban environment", *Proceedings of the 14th International Conference on Soil Mechanics and Foundation Engineering*, Vol. 4, pp. 2353-2385.

Mair, R.J., Gunn, M.J. and O'Reilly, M.P. (1981), "Centrifugal testing of model tunnels in soft clay", *Proceedings of the 10th International Conference on Soil Mechanics and Foundation Engineering*, Vol. 1, pp. 323-328.

Marji, M.F. (2015), "Simulation of crack coalescence mechanism underneath single and double disc cutters by higher order displacement discontinuity method", *J. Central South Univ.*, **22**(3), 1045-1054. https://doi.org/10.1007/s11771-015-2615-6

Marji, M., Hosseini Nasab, H. and Hossein Morshedi, A. (2009), "Numerical modeling of crack propagation in rocks under TBM disc cutters", *J. Mech. Mater. Struct.*, **4**(3), 605-627. https://doi.org/10.2140/jomms.2009.4.605

Melis, M., Medina, L. and Rodríguez, J.M. (2002), "Prediction and analysis of subsidence induced by shield tunnelling in the Madrid Metro extension", *Can. Geotech. J.*, **39**(6), 1273-1287. https://doi.org/10.1139/t02-073

Mirsalari, S.E., Fatehi Marji, M., Gholamnejad, J. and Najafi, M. (2017), "A boundary element/finite difference analysis of subsidence phenomenon due to underground structures", *J. Mining Environ.*, **8**(2), 237-253. https://doi.org/10.22044/JME.2016.759

Monfared, M.M. (2017), "Mode III SIFs for interface cracks in an FGM coating-substrate system", *Struct. Eng. Mech., Int. J.*, **64**(1), 78-95. https://doi.org/10.12989/sem.2017.64.1.071

Nabil, B., Abdelkader, B., Miloud, A. and Noureddine, B. (2012), "On the mixed-mode crack propagation in FGMs plates: comparison of different criteria", *Struct. Eng. Mech., Int. J.*, **61**(3), 201-213. https://doi.org/10.12989/sem.2017.61.3.371

Neaupane, K.M. and Adhikari, N. (2006), "Prediction of tunnelinginduced ground movement with the multi-layer perceptron", *Tunnel. Undergr. Space Technol.*, **21**(2), 151-159. https://doi.org/10.1016/j.tust.2005.07.001

Ng, C.W., Shi, J. and Hong, Y. (2013), "Three-dimensional centrifuge modeling of basement excavation effects on an existing tunnel in dry sand", *Can. Geotech. J.*, **50**(8), 874-888. https://doi.org/10.1139/cgj-2012-0423

Nikadat, N. and Marji, M.F. (2016), "Analysis of stress distribution around tunnels by hybridized FSM and DDM considering the influences of joints parameters", *Geomech. Eng., Int. J.*, **11**(2), 269-288. https://doi.org/10.12989/gae.2016.11.2.269

Nikadat, N., Fatehi, M. and Abdollahipour, A. (2015), "Numerical modelling of stress analysis around rectangular tunnels with large discontinuities (fault) by a hybridized indirect BEM", *J. Central South Univ.*, **22**(11), 4291-4299. https://doi.org/10.1007/s11771-015-2977-9

O'Reilly, M.P. and New, B.M. (1982), "Settlements above tunnels in the United Kingdom—Their magnitude and prediction", *Tunnelling '82. Proceedings of the 3rd International Symposium, Institution of Mining & Metallurgy*, London, UK, pp. 173-181.

Oda, M. and Kazama, H. (1998), "Microstructure of shear bands and its relation to the mechanisms of dilatancy and failure of dense granular soils", *Geotechnique*, **48**(4), 465-481. https://doi.org/10.1680/geot.1998.48.4.465

Ou, C.-Y., Teng, F.-C. and Wang, I.-W. (2008), "Analysis and design of partial ground improvement in deep excavations", *Comput. Geotech.*, **35**(4), 576-584. https://doi.org/10.1016/j.compgeo.2007.09.005

Pan, B., Gao, Y. and Zhong, Y. (2014), "Theoretical analysis of overlay resisting crack propagation in old cement concrete pavement", *Struct. Eng. Mech., Int. J.*, **52**(4) 167-181. https://doi.org/10.12989/sem.2014.52.4.829

Panaghi, K., Golshani, A. and Takemura, T. (2015), "Rock failure assessment based on crack density and anisotropy index variations during triaxial loading tests", *Geomech. Eng., Int. J.*, **9**(6), 793-813. https://doi.org/10.12989/gae.2015.9.6.793

Papastamos, G., Stiros, S., Saltogianni, V. and Kontogianni, V. (2014), "3-D strong tilting observed in tall, isolated brick chimneys during the excavation of the Athens Metro", *Appl. Geomatics*, **7**(2), 115-121. https://doi.org/10.1007/s12518-014-0138-8

Park, K. (2004), "Elastic solution for tunneling-induced ground movements in clays", *Int. J. Geomech.*, **4**(4), 310-318. https://doi.org/10.1061/(ASCE)1532-3641(2004)4:4(310)

Peck, R.B. (1969), "Deep excavations and tunneling in soft ground", *Proceedings of the 7th International Conference on Soil Mechanics and Foundation Engineering*, Mexico, pp. 225-290.

PFC 2D (particle flow code in two dimensions) (1999), version 1.1. Itasca Consulting Group; Inc., Minneapolis, MN, USA, ICG.

Potyondy, D.O. and Cundall, P.A. (2004), "A bounded-particle model for rock", *Int. J. Rock Mech. Min. Sci.*, **41**(8), 1329-1364. https://doi.org/10.1016/j.ijrmms.2004.09.011

Ramadoss, P. and Nagamani, K. (2013), "Stress-strain behavior and toughness of high-performance steel fiber reinforced concrete in compression", *Comput. Concrete, Int. J.*, **11**(2), 55-65. https://doi.org/10.12989/cac.2013.11.2.149

Rothenburg, L. and Bathurst, R.J. (1989), "Analytical study of induced anisotropy in idealized granular materials", *Geotechnique*, **39**(4), 601-614. https://doi.org/10.1680/geot.1989.39.4.601

Suwansawat, S. and Einstein, H.H. (2006), "Artificial neural networks for predicting the maximum surface settlement caused by EPB shield tunneling", *Tunnel. Undergr. Space Technol.*, **21**(2), 133-150. https://doi.org/10.1016/j.tust.2005.06.007

Wan, M.S.P., Standing, J.R., Potts, D.M. and Burland, J.B. (2016), "Measured short-term ground surface response to EPBM tunneling in London Clay", *Geotechnique*, **67**(5), 420-445. https://doi.org/10.1680/jgeot.16.P.099

Wang, F., Gou, B. and Qin, Y. (2013), "Modeling tunneling-induced ground surface settlement development using a wavelet smooth relevance vector machine", *Comput. Geotech.*, **54**(1), 125-132. https://doi.org/10.1016/j.compgeo.2013.07.004

Wu, X., Liu, H., Zhang, L., Skibniewski, M.J., Deng, Q. and Teng, J. (2015), "A dynamic Bayesian network based approach to safety decision supportintunnelconstruction", *Reliab. Eng. Syst. Safe.*, **134**(1), 157-168. https://doi.org/10.1016/j.ress.2014.10.021

Yoo, C. and Lee, D. (2008), "Deep excavation-induced ground surface movement characteristics—A numerical investigation", *Comput. Geotech.*, **35**(2), 231-252. https://doi.org/10.1016/j.compgeo.2007.05.002

Zhang, L., Wu, X., Chen, Q., Skibniewski, M.J. and Zhong, J. (2015), "Developing a cloud model based risk assessment methodology for tunnel-induced damage to existing pipelines", *Stochastic Environ. Res. Risk Assess.*, **29**(2), 513-526. https://doi.org/10.1007/s00477-014-0878-3

Zhou, X.P. and Bi, J. (2018), "Numerical simulation of thermal cracking in rocks based on general particle dynamics", *J. Eng. Mech.*, **144**(1), 04017156. https://doi.org/10.1061/(ASCE)EM.1943-7889.0001378

CC